Anti-Counterfeiting

Wide-Range Color-Tunable Organic Phosphorescence Materials for Printable and Writable Security Inks

Yunxiang Lei[+], Wenbo Dai[+], Jianxin Guan[+], Shuai Guo, Fei Ren, Yudai Zhou, Jianbing Shi, Bin Tong, Zhengxu Cai,* Junrong Zheng, and Yuping Dong*

Abstract: Organic materials with long-lived, color-tunable phosphorescence are potentially useful for optical recording, anti-counterfeiting, and bioimaging. Herein, we develop a series of novel host–guest organic phosphors allowing dynamic color tuning from the cyan (502 nm) to orange red (608 nm). Guest materials are employed to tune the phosphorescent color, while the host materials interact with the guest to activate the phosphorescence emission. These organic phosphors have an ultra-long lifetime of 0.7 s and a maximum phosphorescence efficiency of 18.2 %. Although color-tunable inks have already been developed using visible dyes, solution-processed security inks that are temperature dependent and display time-resolved printed images are unprecedented. This strategy can provide a crucial step towards the next-generation of security technologies for information handling.

Introduction

Purely organic room-temperature phosphorescence (RTP) materials with long-lived, persistent luminescence in the visible spectrum are applicable in optical recording, anti-counterfeiting, and high contrast background independent bioimaging.[1] Fundamental understanding of the luminescence process through molecular design is the central theme of organic RTP. A seemingly general strategy is to enhance the intersystem crossing (ISC) from the singlet state to triplet state.[2] Therefore, most traditional RTP materials are carbazole or phenothiazine based donor (D)-acceptor (A) small molecules with a distorted configuration.[2,3] The intramolecular D–A interaction can narrow the energy gap between the lowest singlet and triplet state (ΔE_{ST}).[4] Aldehyde group and halogens can also be introduced into small molecules to increase the spin-orbit coupling (SOC) constant.[4a,5] Small ΔE_{ST} and large SOC constant are conducive to enhance the ISC ability of excition.[2–4] However, this molecular design strategy faces several urgent issues, such as short phosphorescence wavelengths, low brightness, and lack of new systems.[1d–g,2,3]

Recently, a novel method to generate RTP was reported by embedding guest materials into a rigid or crystalline host matrix, such as steroid analogue, the cavity of cyclodextrin, poly(vinyl alcohol), and poly(methyl methacrylate).[6] The rigidity of the matrix avoids quenching of the triplet excitons by interactions with the humidity and oxygen.[6a,c,e] In addition, the rigid host also restricts the molecular motion of the guest molecules, thereby promoting their phosphorescence.[6a,b,e] However, the major role of the matrix molecules in the multi-component RTP system remains elusive. Researchers still need to carefully choose the matrix for a guest phosphor. A rigid or crystalline matrix is unsuitable for all guest phosphors, resulting in a lack of wide range color tunable RTP materials.[6a,c–e] Tunable emission color endows RTP materials with superior performance in optoelectronic applications. For instance, multicolor-encoded materials can serve as information carriers for encrypted data storage, high-density, and anti-counterfeiting.[7] Furthermore, long wavelength RTP materials are ideal biomarkers for bioimaging.[8] To date, the development of wide-range color-tunable emission RTP materials remains a formidable challenge, which greatly limits application of multi-component phosphorescence materials.[1b,h,6f,g]

Herein, we demonstrate a host–guest doping approach that can achieve wide-range color tuning of RTP emission. Both the host and guest molecules have no phosphorescence at the room temperature. When the guest molecules were doped into the host molecules, maximum phosphorescent quantum yield reaches 18.2 %. The experimental results also reveal that the host molecules not only restrict the motion of the guest molecules, but also show a synergistic effect to the guest at excited state. The host materials of both triphenylphosphine (**TPP**) and triphenylarsenic (**TPAs**) exhibit low melting points and highly stable subcooling states. Therefore, the host-guest RTP system can be solution-processed in both molten state and solution state. The hand-writing characters of RTP inks and printing Figure by the ink solution display similar color under sunlight and UV light, but show a dynamic color change after removal of UV light. In addition, RTP performance of the host-guest materials at high temperature is highly dependent on guest molecules. The three-component RTP system possesses a phosphorescent thermochromic

[*] Y. Lei,[+] W. Dai,[+] S. Guo, F. Ren, Y. Zhou, Prof. J. Shi, Prof. B. Tong, Prof. Z. Cai, Prof. Y. Dong
Beijing Key Laboratory of Construction Tailorable Advanced Functional Materials and Green Applications, School of Materials Science & Engineering, Beijing Institute of Technology
Beijing 100081 (China)
E-mail: caizx@bit.edu.cn
        chdongyp@bit.edu.cn
J. Guan,[+] Prof. J. Zheng
Beijing National Laboratory for Molecular Sciences, College of Chemistry and Molecular Engineering, Peking University
Beijing 100871 (China)

[+] These authors contributed equally to this work.

Supporting information and the ORCID identification number(s) for the author(s) of this article can be found under:
https://doi.org/10.1002/anie.202003585.
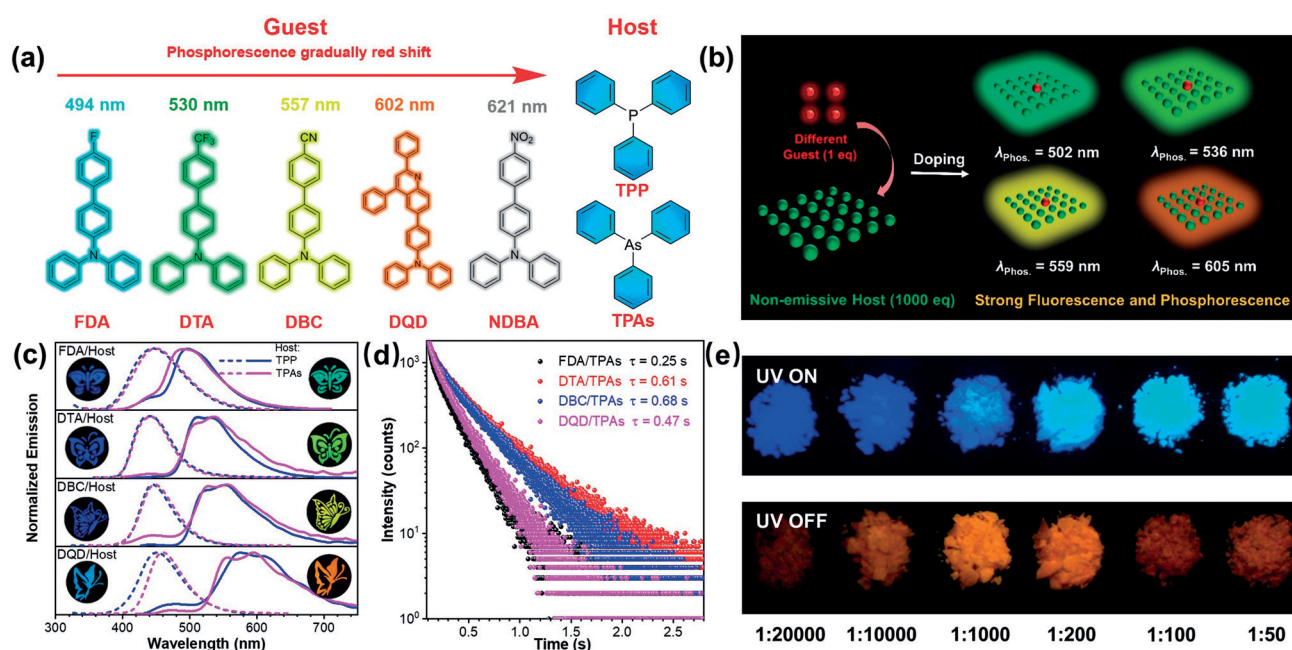
Figure 1. a) The molecular structures of guest and host molecules. b) Schematic diagram of host–guest phosphorescence materials. c) Fluorescence (dash line) and phosphorescence (solid line) spectra of host–guest crystalline materials. Inset: photographs of guest/**TPAs** materials with and without UV irradiation. d) Phosphorescence decay curves of host–guest materials with **TPAs** as the host, excitation wavelength: 370 nm. e) The fluorescence (top) and phosphorescence (down) images of the **DQD/TPAs** crystalline powders with different amount of **DQD** (Molar ratio).

property. Therefore, multiple dimensional, including color tunable, temperature dependent, and time-resolved, anti-counterfeiting techniques are achieved in the printable and writable host-guest inks.

Results and Discussion

Figure 1a shows the molecular structures of the hosts and guests. **TPP** and **TPAs** were selected as the host molecules according to our previous results because triphenylamine (**TPA**) displayed good host capacity for **TPA**-based RTP guest materials. Since nitrogen, phosphorus and arsenic are in the same main element group, and heavy atom facilitates the intersystem crossing, **TPP** and **TPAs** as the host materials were expected to process enhanced RTP performance than **TPA**. Four **TPA**-based molecules with electron withdrawing groups (Figure 1a) were designed and synthesized as the guests (Schemes S1 and S2 in the Supporting Information). Both **TPP** and **TPAs** have low melting points (Figure S2, 81.7 °C for **TPP** and 63.1 °C for **TPAs**) and stable subcooling states. Therefore, the guests dispersed in the host can be fabricated by the melt-casting method, in which blends of the materials are simply heated by hot water. All host-guest materials show visible afterglow after removal of irradiation, indicating the present of RTP properties. The concentration of the guest molecules play an important role in the performance of RTP.[9] Therefore, a series of host–guest materials with molar ratio of **DQD** to **TPAs** ranging from 1:50 to 1:20000 were prepared (Figure 1e). As ratio of **DQD** increases, the emission wavelength of the host-guest materials

slightly red shift (Figure S4), likely due to the molecular aggregation of the guest molecules at high concentration.[9a] Notably, even the concentration of **DQD** is as low as 0.005 mol % (1:20000), the host–guest materials still produce obvious visible afterglow. To our knowledge, this value is the lowest guest concentration found in organic host-guest materials that can achieve RTP.

The melt-casting host–guest materials with 0.1 mol % guests dispersed in either **TPP** or **TPAs** exhibiting the best fluorescence and phosphorescence performance were selected for the photophysical investigation. The host–guest materials produce blue fluorescence emission with the wavelength ranging from 433 to 462 nm (Figure 1c, Table 1). The phosphorescence wavelengths of the host–guest materials gradually increase from 502 to 608 nm, achieving full emission coverage from cyan, to green, to yellow, and to orange-red (Figure 1c, Table 1). In addition, eight host–guest crystalline materials all exhibit high luminescent efficiency with phosphorescence quantum yields (Q.Y.) between 8% and 18%, and fluorescence Q.Y. higher than 70% (Table 1). The strong luminous ability of host-guest materials indicates that the host materials restrict the non-radiation transition, thus increasing the light conversion efficiency. On the basis of the RTP-decay curves, the phosphorescence lifetimes of doped crystalline powders ranging from 0.22–0.70 s (Figure 1d and Figure S3c, Table 1), result in multicolor afterglow that last as long as 2–4 s under ambient conditions (Figure S5). In addition, the phosphorescence intensities of **TPAs** based materials are stronger than those of the **TPP** based materials (Table 1), likely due to the heavy atomic effect of arsenic. To calculate the triplet gap between T_1 to ground state of the guest

Table 1: Photophysical properties of host–guest materials.[a]

Sample	Fluo.			Phos.		
	λ_{em} [nm]	Φ_F [%]	τ [ns]	λ_{em} [nm])	Φ_P [%]	τ [s]
FDA/TPP	433	82.5	2.8	502	8.1	0.22
DTA/TPP	438	77.3	2.8	531	16.2	0.58
DBC/TPP	448	81.2	2.5	556	12.8	0.70
DQD/TPP	459	82.8	2.2	608	9.3	0.46
FDA/TPAs	434	80.9	3.2	504	9.2	0.25
DTA/TPAs	442	78.6	3.0	536	18.2	0.61
DBC/TPAs	448	77.6	2.1	559	15.5	0.68
DQD/TPAs	462	78.4	2.0	605	10.9	0.47

[a] Note: Guest: Host = 1:1000 (Molar ratio). Excitation wavelength: 370 nm. All samples are in the crystalline states.

molecules, phosphorescence spectra of the guests were measured in toluene solution at 77 K (Figure S1c). The results indicate that ΔE_{ST} of the guest in host-guest systems are smaller than the guests in toluene (Table S1). The smaller energy gap obviously facilitates the intersystem crossing of excitons, resulting in strong phosphorescence emissions of the host–guest systems at room temperature.[2,3] The color tunable property of host–guest materials provides an opportunity for constructing the white phosphorescence materials with two complementary emission of blue and yellow. **FDA**, **DBC** and **DQD** with **TPAs** (molar ratio: 1:1:1:1000) show a broad phosphorescence peak from 490 to 580 nm (Figure S6a). The Commission Internationale de L'Eclairage (CIE) chromaticity coordinate of **FDA-DBC-DQD/TPAs** powder was calculated as (0.31, 0.38; Figure S6c), which is a bright cold white phosphorescence emission.

Generally, host molecules provide a rigid environment to avoid the quenching of the triplet excitons by interaction with oxygen.[6a–e] However, the degassed **DQD/TPP** (0.1 mol%) molten solution at 85°C and room temperature (subcooling state) only show fluorescence but no phosphorescence (Figure 2). When the host–guest system begins to solidify, the fluorescence of **DQD/TPP** was enhanced and bright phosphorescence was generated (Figure 2). Therefore, the rigid host molecules not only play a role to avoid the quenching of the triplet excitons by oxygen, but also can restrict the motion of the guest molecules and decrease the non-radiation transitions.

Tunable emission color produces RTP materials that exhibit superior performance in bioimaging. Especially the materials with long emission wavelength display low photo-toxicity and high penetrability for cells and tissues.[8,10] Therefore, RTP materials with long emission wavelength were achieving by our host-guest doping strategy. **DQD** guest molecules show a broad phosphorescence peak with a wavelength around at 600 nm at 77 K (Figure S1c), affording phosphorescence emission of 605 nm in **DQD/TPAs** powder. However, the material with a phosphorescence longer than 605 nm were failed to achieve in our host-guest system. For example, **TPA** based molecule with a nitro group which has stronger electron-withdrawing ability as the acceptor, namely, 4′-nitro-*N,N*-diphenyl-[1,1′-biphenyl]-4-amine (**NDBA**, Figure 1a), display a phosphorescence emission at 625 nm at 77 K (Figure S7b). Unexpectedly, **TPAs** materials with any amount of **NDBA** produce only fluorescence, but non-phosphorescence (Figure S7d). Hence, **TPA**-based guest materials with longer emission wavelength will not be suitable for **TPP** and **TPAs** based host–guest systems. Density func-
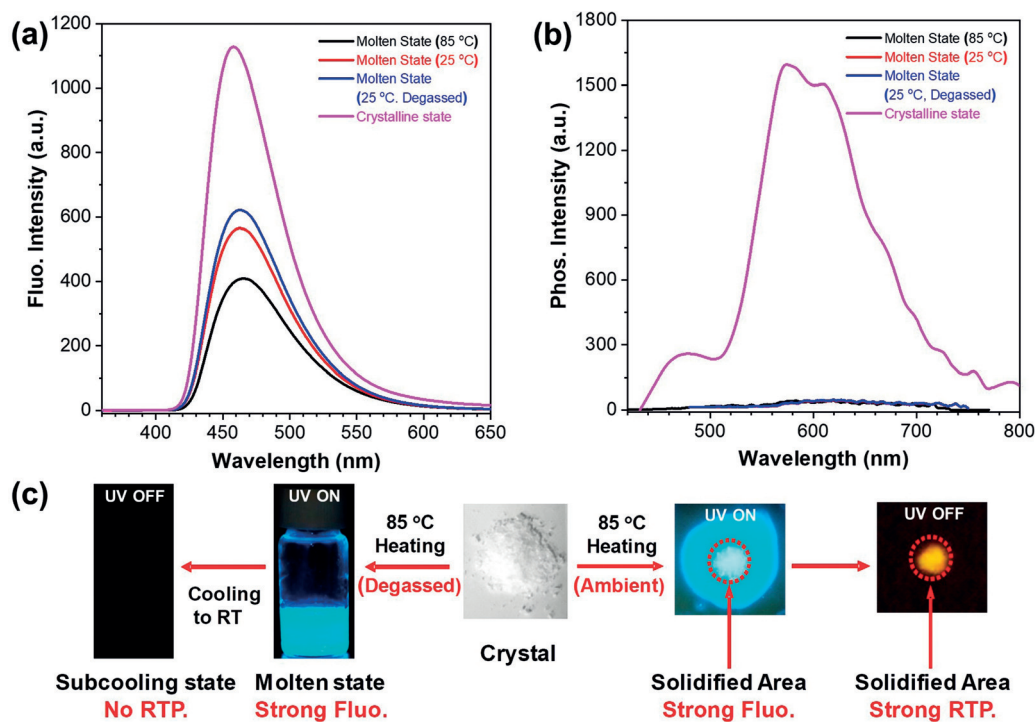
Figure 2. a) Fluorescence spectra of **DQD/TPP**. b) Phosphorescence spectra of **DQD/TPP**. c) Photographs of **DQD/TPP** in different state.

tional theory (DFT) calculations were carried out to offer further insight into host–guest systems. Large band gap between the S_1 and T_1 in guest molecules do not facilitate to the intersystem crossing (Figure 3a).[2,3,11] Therefore, non-phosphorescence was observed in guest powders. T_1 of the host can be the bridge between the S_1 and T_1 of the guest molecules (Figure 3a). However, the large energy gap between T_1 of **TPAs** and T_1 of **NDBA** were not suitable for intermolecular energy transfer (Figure 3b).[12] The host can only restrict the molecular motion of **NDBA** and results in an enhanced fluorescence. The host with low T_1 energy level is needed for pursuing long wavelength emission RTP materials.

The solid-state UV-absorption experiments of **DQD/TPAs** and **NDBA/TPAs** were carried out to confirm the intermolecular interaction between the host and guest. The maximum absorption wavelength of **DQD/TPAs** shows a significant red shift compared to **DQD** powder, indicating the absence of the intermolecular charge transfer between the **DQD** and **TPAs** (Figure 4a). However, the maximum absorption wavelength of **NDBA/TPAs** is almost identical to **NDBA** powder due to lack of intermolecular interaction (Figure 4b). The solvatochromic experiments of **DQD** were performed in different solvents. Compared to the fluorescence spectra of **DQD** in common solvents, **DQD** shows a shorter emission wavelength in the molten host (Figure S9a), indicating that the molten host with a low polarity showed a weak solvent effect. However, the maximum excitation and absorption wavelengths in the molten host are longer than those in common solvents (Figures S9b,c). Hence, the molten host not only acts as the solvent, but also displays a strong interaction with the guest.

To further investigate the host–guest interaction, waiting time-dependent spectra of **TPAs** host, five guests and corresponding host–guest materials were measured (guest and host molar ratio = 1:10 000; excitation wavelength: 370 nm). Transient infrared (IR)-absorption spectra and vibrational relaxation kinetics of five guests are presented in Figure S11 and S12. The absorption peaks of solid samples (1375–1625 cm^{-1}) correspond to benzene skeleton vibration

modes. Upon excitation, the molecules reach high vibrational level of their excited states without conformation changes, according to the Frank-Condon principle.[13] Then the excited molecules relax back to the ground state via vibration relaxation from excited vibrational level to the ground vibrational level. The fast relaxation lifetime, within 2 ps (Figure S12), are heavily distorted by nonlinear effects arising from the temporal overlap of the pump and probe pulse, at the first several picoseconds of our decay signal.[14] All the guest molecules exhibit the similar vibrational lifetimes ranging from 120 to 170 ps, whereas the vibrational lifetime of the **TPAs** is only 62 ps, which is significantly shorter than those of the guest molecules (Figure S12). Since the maximum absorption wavelength red shifts from 321 nm to 407 nm from **FDA** to **NDBA** (Figure S8a), and **DQD** shows the maximum molar absorption coefficient at 370 nm, **DQD** possesses the highest excitation efficiency. The broad absorption in the transient IR-absorption spectra illustrates that the free electron moves among solid molecules.[15] In addition, all guest molecules show a long-lived process, where the persistent mid-IR absorption may arise from a population of singlet excited state that cannot undergo singlet decay, probably due to singlet trapping or disorder in the films.

Transient IR-absorption spectra of five host–guest materials are presented in Figure 4g–k. **TPAs** show a strong absorption peak with an excitation wavelength at 280 nm, but almost no absorption peak under 370 nm excitation (Figures 4d–f). However, when the four host–guest materials are excited by an excitation source at 370 nm, **TPAs** molecules display relatively strong absorption peaks (Figures 4g–j). Once the guest molecules are excited, the excitation energy can transfer from the guest to the host, indicating the existence of intermolecular interaction between these molecules. The vibrational lifetimes of the host in host-guest materials are three-fold longer than that of pure host molecule excited under 280 nm (Figure 4c, Figure S13). In addition, the interaction between **DBC** to **TPAs** is strongest among the four host–guest materials, which is consistent with the fact that **DBC/TPAs** has the longest phosphorescence lifetime. Furthermore, the **NDBA/TPAs** with non-RTP phenomenon shows an extremely weak absorption signal in transient IR-absorption measurement (Figure 4k). Therefore, the rigid host is not only used to minimize oxygen effects and restrict the motion of the guest molecules on the phosphorescence processes. A synergistic interaction between the host and guest is an indispensable factor for the realization of RTP in host–guest system.

The vibrational freedoms of host–guest systems are largely affected by noncryogenic temperature changes below their melting points. This phenomenon offers the possibility of enhancing the effect of temperature on phosphorescence intensity. The phosphorescence intensity of **FDA/TPP, DTA/TPP, DBC/TPP, DQD/TPP** quench by 96%, 85%, 36%, 21%, respectively, when the temperature increases from 15 to 65°C (Figure 5a and Figure S14). The difference in intensity quenching can be attributed to the difference in vibrational freedoms between the host and guest. Strong electron withdrawing substitute promotes strong host–guest interaction, thus decreasing the molecular vibration. As shown in Fig-
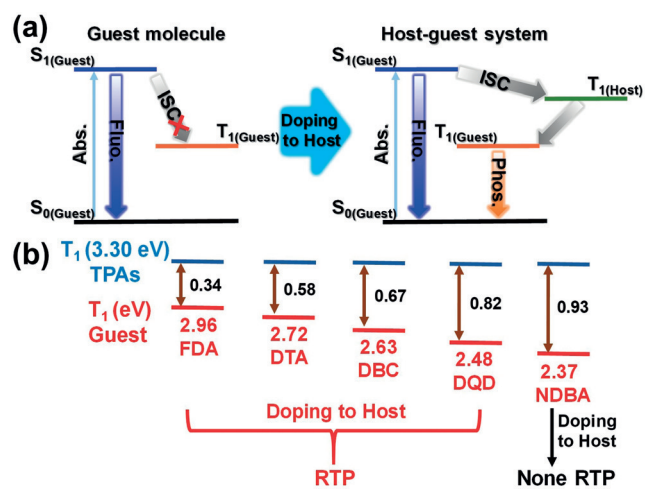
Figure 3. a) Proposed energy-transfer path between guest and host. b) The energy levels of the **TPAs** and the guests.
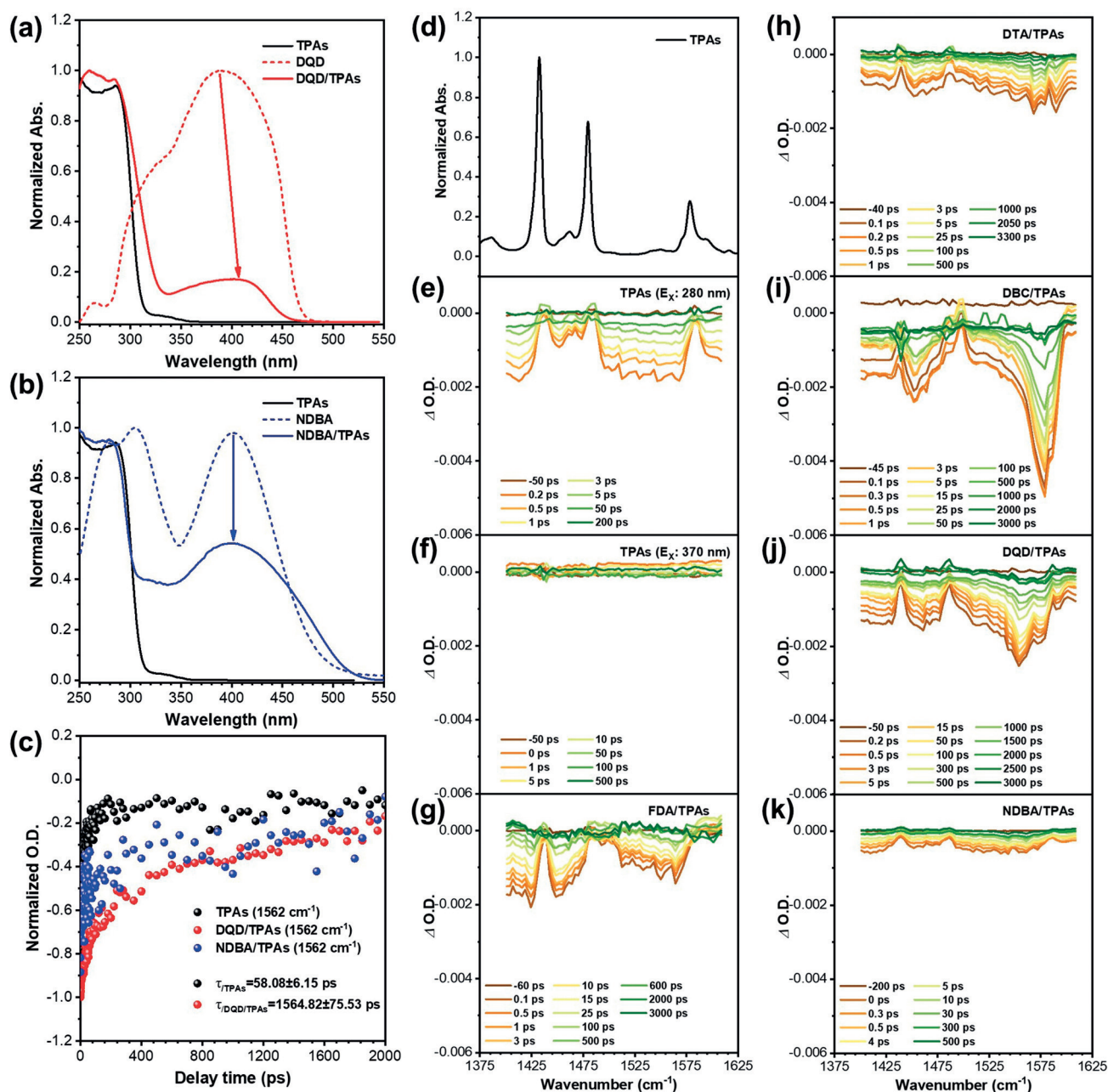
Figure 4. a) UV absorption spectra of **TPAs**, **DQD**, and **DQD/TPAs**. b) UV absorption spectra of **TPAs**, **NDBA**, and **NDBA/TPAs**. c) The vibrational relaxation kinetics of **TPAs**, **DQD/TPAs**, **NDBA/TPAs** (**TPAs**, excitation wavelength: 280 nm. **DQD**/**TPAs** and **NDBA**/**TPAs**, excitation wavelength: 370 nm). O.D. = optical density. d) IR-absorption of **TPAs**. e) Transient IR-absorption spectra of **TPAs**, excitation wavelength: 280 nm. f) Transient IR-absorption spectra of **TPAs**, excitation wavelength: 370 nm. g)–k) Transient IR-absorption spectra of five host–guest materials, excitation wavelength: 370 nm.

ure 5b, the pattern displays different information at different temperatures, which can be exploited for thermochromic anti-counterfeiting. Three-component host–guest material of **DTA-DQD/TPP** (molar ratio: 1:1:1000) was also prepared for the investigation of phosphorescent thermochromic property. **DTA-DQD/TPP** shows green phosphorescence at 15°C due to high phosphorescence Q.Y. of **DTA/TPP**. As the temperature increases, a dramatic decrease in phosphorescence intensity of **DTA/TPP** and slight decrease in phosphorescence intensity of **DQD/TPP** are observed. Therefore, the

phosphorescence wavelength of **DTA-DQD/TPP** gradually red-shift to orange with increasing temperature (Figure 5c,e). The in situ phosphorescence spectra of the heating and cooling in the temperature range of 15–65°C was recorded in order to monitor the thermal response reversibility. Reversible phosphorescence is repeated in four consecutive cycles, indicating that thermochromic anti-counterfeiting that utilize this system can be reusable (Figure 5d). The host-guest materials can be easily heated to the molten state (85°C) as the ink for calligraphy with the writing brushes. As shown in
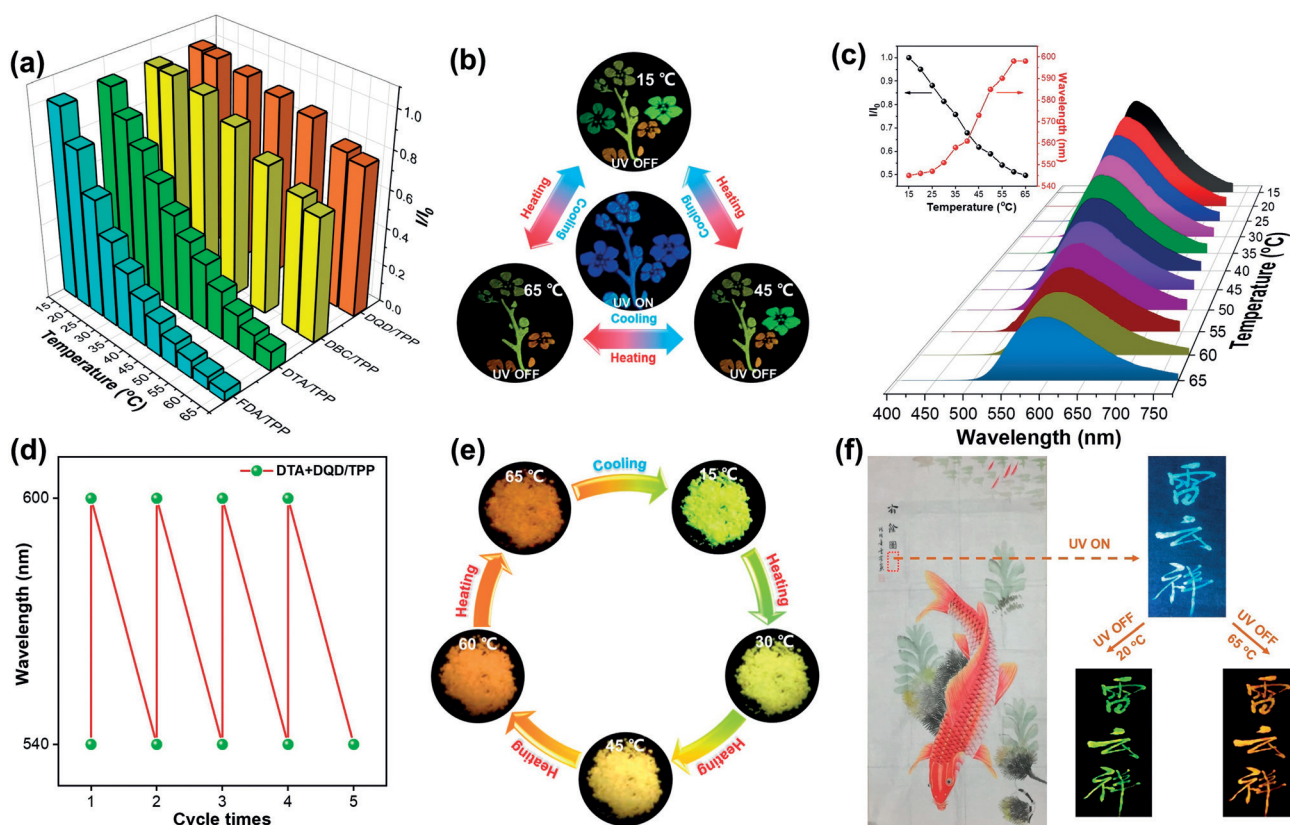
Figure 5. a) In situ phosphorescence intensity of host–guest materials in the temperature range of 15–65 °C. b) Photographs of the flower before (in the middle) and after removing the excitation source at different temperatures. c) Phosphorescence wavelength and intensity of **DTA-DQD/TPP** materials at different temperatures. d) In situ phosphorescence wavelength of **DTA-DQD/TPP** materials during four cycles. e) Phosphorescence color of **DTA-DQD/TPP** host–guest material at different temperatures. f) Application of **DTA-DQD/TPP** in anti-counterfeiting of calligraphy and artworks.

Figure 5 f, the characters show a bright cyan fluorescence under UV-radiation. After removing the excitation source, the characters display green phosphorescence at room temperature. Slight heating results in a bright orange afterglow. Therefore, the time-resolved thermochromic property of **DTA-DQD/TPP** can be explored as sensitive, inert, and cheap materials for anti-counterfeiting.

The counterfeiting of currency, valuable documents, and branded commodities has become a challenging issue that has serious economic, security and health ramifications for governments and businesses.[16] Therefore, the development of security inks that are not able to be photocopied, but are readable only under special conditions has become of increasing importance. In addition to be used as the security inks at subcooling state, our host–guest materials are also considered to be conjoined with a facile process, such as writing and printing in solution state. The filter paper can be first soaked with the molten host molecules. The guest molecules can be dissolved in their good solvents, such as CH_2Cl_2 (DCM) or tetrahydrofuran at a concentration of 1×10^{-4} mol L^{-1}. Furthermore, various complicated patterns have been written or printed with good resolution by using guest solution (Figure S16). As shown in Figure S16a, a butterfly was drawn with four types of guest inks. After thorough drying under ambient conditions, it is invisible under ambient light. Upon irradiation with 365 nm UV lamp, a bright blue

pattern emerges due to similar fluorescence of the four guest–host system. In addition, the butterfly changes to a brilliant colorful self-protective RTP after removal of the UV lamp. The security badge was also printed on A4 paper using an ijd300 printer where a vacant black cartridge is injected with guest solutions (1×10^{-4} mol L^{-1} in DCM). As shown in Figure S16b, the information on the badge was invisible both under ambient light and under UV light due to the strong fluorescence background of the A4 paper (Figure S15). The colorful information, including the portrait, the name, the organization, and the badge number is readable after removal the irradiation. Therefore, the information on the badge can only be read and identified, but cannot be photocopied and duplicated even when was stolen. Notably, the long-lived afterglow phenomenon with color tunable, temperature-dependent, and time-resolved properties provides a very high level of security application for protecting the authenticity of many important and valuable items.

Conclusion

In conclusion, we developed a series of host–guest materials with RTP properties. The phosphorescence color can be tuned from 502 to 608 nm under ambient conditions by selecting different guests. This opens up a broad class of pure

organic compounds to new applications in phosphor design. In light of both the experimental results and simulation, we believe that the host molecules can not only restrict the molecular motion and avoid the triplet quenching from the oxygen, but also interact for the realization of RTP. These materials with color tunable, temperature dependent, and time-resolved emissive properties can be used as writable and printable inks for multiple-dimensional anti-counterfeiting.

Acknowledgements

Conflict of interest

The authors declare no conflict of interest.

[1] a) O. Bolton, K. Lee, H. J. Kim, K. Y. Lin, J. Kim, *Nat. Chem.* **2011**, *3*, 205–210; b) L. Gu, H. Shi, L. Bian, M. Gu, K. Ling, X. Wang, H. Ma, S. Cai, W. Ning, L. Fu, H. Wang, S. Wang, Y. Gao, W. Yao, F. Huo, Y. Tao, Z. An, X. Liu, W. Huang, *Nat. Photonics* **2019**, *13*, 406–411; c) Y. Xiong, Z. Zhao, W. Zhao, H. Ma, Q. Peng, Z. He, X. Zhang, Y. Chen, X. He, J. W. Y. Lam, B. Z. Tang, *Angew. Chem. Int. Ed.* **2018**, *57*, 7997–8001; *Angew. Chem.* **2018**, *130*, 8129–8133; d) Z. An, C. Zheng, Y. Tao, R. Chen, H. Shi, T. Chen, Z. Wang, H. Li, R. Deng, X. Liu, W. Huang, *Nat. Mater.* **2015**, *14*, 685–690; e) Z. He, H. Gao, S. Zhang, S. Zheng, Y. Wang, Z. Zhao, D. Ding, B. Yang, Y. Zhang, W. Z. Yuan, *Adv. Mater.* **2019**, *31*, 1807222; f) W. Zhao, Z. He, J. W. Y. Lam, Q. Peng, H. Ma, Z. Shuai, G. Bai, J. Hao, B. Z. Tang, *Chem* **2016**, *1*, 592–602; g) G. Zhang, G. M. Palmer, M. W. Dewhirst, C. L. Fraser, *Nat. Mater.* **2009**, *8*, 747–751; h) J. Zhao, W. Wu, J. Sun, S. Guo, *Chem. Soc. Rev.* **2013**, *42*, 5323–5351.

[2] a) H. Ma, Q. Peng, Z. An, W. Huang, Z. Shuai, *J. Am. Chem. Soc.* **2019**, *141*, 1010–1015; b) Y. Xie, Y. Ge, Q. Peng, C. Li, Q. Li, Z. Li, *Adv. Mater.* **2017**, *29*, 1606829.

[3] a) T. Wang, X. Su, X. Zhang, X. Nie, L. Huang, X. Zhang, X. Sun, Y. Luo, G. Zhang, *Adv. Mater.* **2019**, *31*, 1904273; b) J. Wang, Z. Chai, J. Wang, C. Wang, M. Han, Q. Liao, A. Huang, P. Lin, C. Li, Q. Li, Z. Li, *Angew. Chem. Int. Ed.* **2019**, *58*, 17297–17302; *Angew. Chem.* **2019**, *131*, 17457–17462; c) Y. Gong, G. Chen, Q. Peng, W. Z. Yuan, Y. Xie, S. Li, Y. Zhang, B. Z. Tang, *Adv. Mater.* **2015**, *27*, 6195–6201; d) C. J. Chen, R. J. Huang, A. S. Batsanov, P. Pander, Y. T. Hsu, Z. G. Chi, F. B. Dias, M. R. Bryce, *Angew. Chem. Int. Ed.* **2018**, *57*, 16407–16411; *Angew. Chem.* **2018**, *130*, 16645–16649.

[4] a) Y. Lei, W. Dai, Z. Liu, S. Guo, Z. Cai, J. Shi, X. Zheng, J. Zhi, B. Tong, Y. Dong, *Mater. Chem. Front.* **2019**, *3*, 284–291; b) Y. Gong, L. Zhao, Q. Peng, D. Fan, W. Z. Yuan, Y. Zhang, B. Z. Tang, *Chem. Sci.* **2015**, *6*, 4438–4444.

[5] a) Y. Shoji, Y. Ikabata, Q. Wang, D. Nemoto, A. Sakamoto, N. Tanaka, J. Seino, H. Nakai, T. Fukushima, *J. Am. Chem. Soc.* **2017**, *139*, 2728–2733; b) Z. He, W. Zhao, J. W. Y. Lam, Q. Peng, H. Ma, G. Liang, Z. Shuai, B. Z. Tang, *Nat. Commun.* **2017**, *8*,

[6] a) J. Wei, B. Liang, R. Duan, Z. Cheng, C. Li, T. Zhou, Y. Yi, Y. Wang, *Angew. Chem. Int. Ed.* **2016**, *55*, 15589–15593; *Angew. Chem.* **2016**, *128*, 15818–15822; b) M. S. Kwon, D. Lee, S. Seo, J. Jung, J. Kim, *Angew. Chem. Int. Ed.* **2014**, *53*, 11177–11181; *Angew. Chem.* **2014**, *126*, 11359–11363; c) D. Li, F. Lu, J. Wang, W. Hu, X. M. Cao, X. Ma, H. Tian, *J. Am. Chem. Soc.* **2018**, *140*, 1916–1923; d) Z. Y. Zhang, Y. Liu, *Chem. Sci.* **2019**, *10*, 7773–7778; e) S. Hirata, K. Totani, J. Zhang, T. Yamashita, H. Kaji, S. R. Marder, T. Watanabe, C. Adachi, *Adv. Funct. Mater.* **2013**, *23*, 3386–3397; f) Y. Su, Y. Zhang, Z. Wang, W. Gao, P. Jia, D. Zhang, C. Yang, Y. Li, Y. Zhao, *Angew. Chem. Int. Ed.* **2020**, *59*, 9967–9971; *Angew. Chem.* **2020**, *132*, 10053–10057; g) Z. Wang, Y. Zhang, C. Wang, X. Zheng, Y. Zheng, L. Gao, C. Yang, Y. Li, L. Qu, Y. Zhao, *Adv. Mater.* **2020**, *32*, 201907355; h) Y. X. Lei, W. B. Dai, Y. Tian, J. H. Yang, P. F. Li, J. B. Shi, B. Tong, Z. X. Cai, Y. P. Dong, *J. Phys. Chem. Lett.* **2019**, *10*, 6019–6025.

[7] a) X. Wang, H. L. Ma, M. X. Gu, C. Q. Lin, N. Gan, Z. L. Xie, H. Wang, L. F. Bian, L. S. Fu, S. Z. Cai, Z. G. Chi, W. Yao, Z. F. An, H. F. Shi, W. Huang, *Chem. Mater.* **2019**, *31*, 5584–5591; b) Q. Mei, Z. Zhang, *Angew. Chem. Int. Ed.* **2012**, *51*, 5602–5606; *Angew. Chem.* **2012**, *124*, 5700–5704; c) C. Zhang, L. Yang, J. Zhao, B. Liu, M. Y. Han, Z. Zhang, *Angew. Chem. Int. Ed.* **2015**, *54*, 11531–11535; *Angew. Chem.* **2015**, *127*, 11693–11697.

[8] S. M. A. Fateminia, Z. Mao, S. Xu, Z. Yang, Z. Chi, B. Liu, *Angew. Chem. Int. Ed.* **2017**, *56*, 12160–12164; *Angew. Chem.* **2017**, *129*, 12328–12332.

[9] a) R. Kabe, C. Adachi, *Nature* **2017**, *550*, 384–387; b) X. Zhang, L. Du, W. Zhao, Z. Zhao, Y. Xiong, X. He, P. F. Gao, P. Alam, C. Wang, Z. Li, J. Leng, J. Liu, C. Zhou, J. W. Y. Lam, D. L. Phillips, G. Zhang, B. Z. Tang, *Nat. Commun.* **2019**, *10*, 5161; c) Z. Lin, R. Kabe, N. Nishimura, K. Jinnai, C. Adachi, *Adv. Mater.* **2018**, *30*, 1803713.

[10] J. Xu, A. Takai, Y. Kobayashi, M. Takeuchi, *Chem. Commun.* **2013**, *49*, 8447–8449.

[11] a) H. Sun, Z. Hu, C. Zhong, X. Chen, Z. Sun, J. L. Brédas, *J. Phys. Chem. Lett.* **2017**, *8*, 2393–2398; b) H. Han, E. G. Kim, *Chem. Mater.* **2019**, *31*, 6925–6935; c) B. L. Cotts, D. G. McCarthy, R. Noriega, S. B. Penwell, *ACS Energy Lett.* **2017**, *2*, 1526–1533.

[12] a) X. Vries, P. Friederich, W. Wenzel, R. Coehoorn, P. A. Bobbert, *Phys. Rev. B* **2019**, *99*, 205201; b) R. Gaoa, D. P. Yan, *Chem. Sci.* **2017**, *8*, 590–599; c) K. Totani, Y. Okada, S. Hirata, M. Vacha, T. Watanabe, *Adv. Opt. Mater.* **2013**, *1*, 283–288; d) X. P. Zhang, L. L. Du, W. J. Zhao, D. Phillips, G. Q. Zhang, B. Z. Tang, *Nat. Commun.* **2019**, *10*, 5161.

[13] J. R. Lakowicz, *Principles of Fluorescence Spectroscopy*, Springer Science & Business Media, Cham, **2013**.

[14] a) J. Zhang, S. Sulaiman, I. K. Madu, R. M. Laine, T. Goodson, *J. Phys. Chem. C* **2019**, *123*, 5048–5060; b) A. Kushnarenko, E. Miloglyadov, M. Quack, G. Seyfang, *Phys. Chem. Chem. Phys.* **2018**, *20*, 10949–10959.

[15] a) L. W. Barbour, M. Hegadorn, J. B. Asbury, *J. Am. Chem. Soc.* **2007**, *129*, 15884–15894; b) O. Varnavski, N. Abeyasinghe, J. Aragó, J. J. Serrano-Pérez, E. Ortí, J. T. López Navarrete, K. Takimiya, D. Casanova, J. Casado, T. Goodson, *J. Phys. Chem. Lett.* **2015**, *6*, 1375–1384.

[16] a) S. Erevelles, N. Fukawa, L. Swayne, *J. Bus. Res.* **2016**, *69*, 897–904; b) X. Liu, Y. Wang, X. Li, Z. Yi, R. Deng, L. Liang, X. Xie, D. T. B. Loong, S. Song, D. Fan, A. H. All, H. Zhang, L. Huang, X. Liu, *Nat. Commun.* **2017**, *8*, 899; c) J. F. Barrera, A. Mira, R. Torroba, *Opt. Express* **2013**, *21*, 5373–5378.